

Supplementary Information

Highly Sensitive and Selective Colorimetric and Off-On Fluorescent Reversible Chemosensors for Al^{3+} Based on the Rhodamine Fluorophore. *Sensors* 2015, 15, 9097–9111

Naveen Mergu ¹, Ashok Kumar Singh ¹ and Vinod Kumar Gupta ^{1,2,3,*}

¹ Department of Chemistry, Indian Institute of Technology Roorkee, Roorkee 247 667, India; E-Mails: mergu.naveen@gmail.com (N.M.); akscyfcy@gmail.com (A.K.S.)

² Center for Environment and Water, The research Institute, King Fahd University of Petroleum & Minerals, Dhahran 31261, Saudi Arabia

³ Department of Applied Chemistry, University of Johannesburg, Johannesburg 17011, South Africa

* Author to whom correspondence should be addressed; E-Mails: vinodfcy@iitr.ac.in or vinodfcy@gmail.com; Tel.: +91-133-2285-801; Fax: +91-133-2273-560.

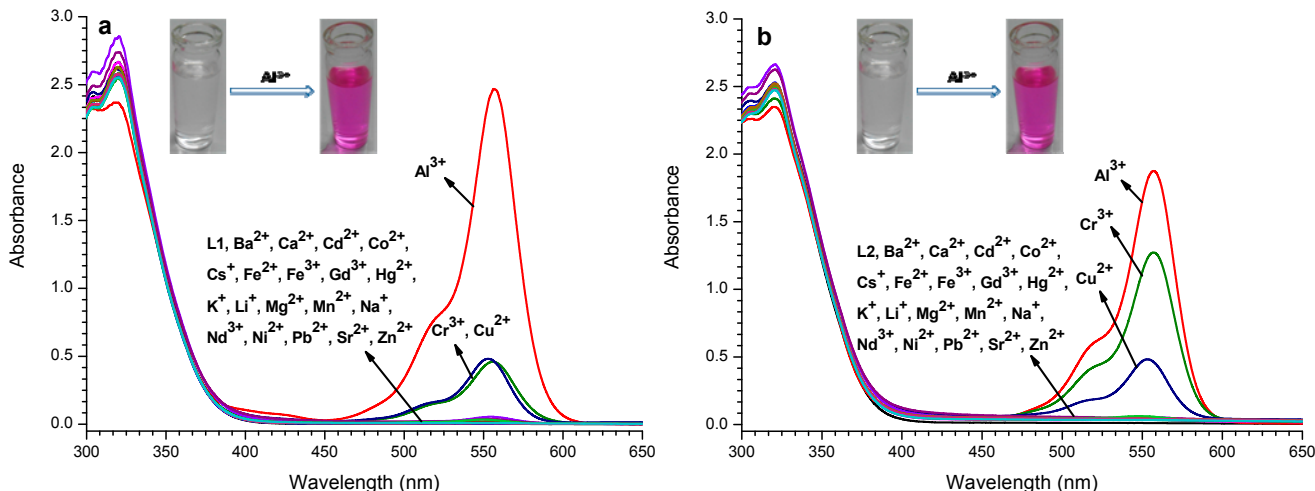


Figure S1. Absorbance spectra of **L1** (**a**, 50 μM) and **L2** (**b**, 50 μM) in presence of various metal ions (50 μM) in MeOH–DMSO (99:1 v/v). Inset: Visual color change of probe upon addition of Al^{3+} .

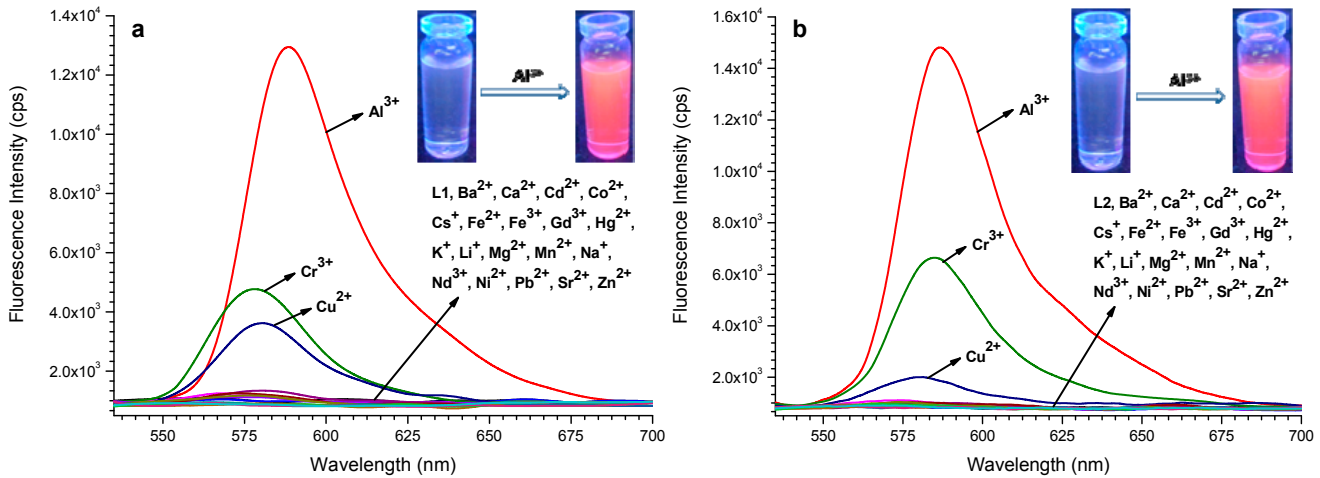


Figure S2. Fluorescence spectra ($\lambda_{\text{ex}} = 520 \text{ nm}$) of **L1** (a, 50 μM) and **L2** (b, 50 μM) in presence of various metal ions (50 μM) in MeOH–DMSO (99:1 v/v). Inset: Visual color change of probe upon addition of Al^{3+} .

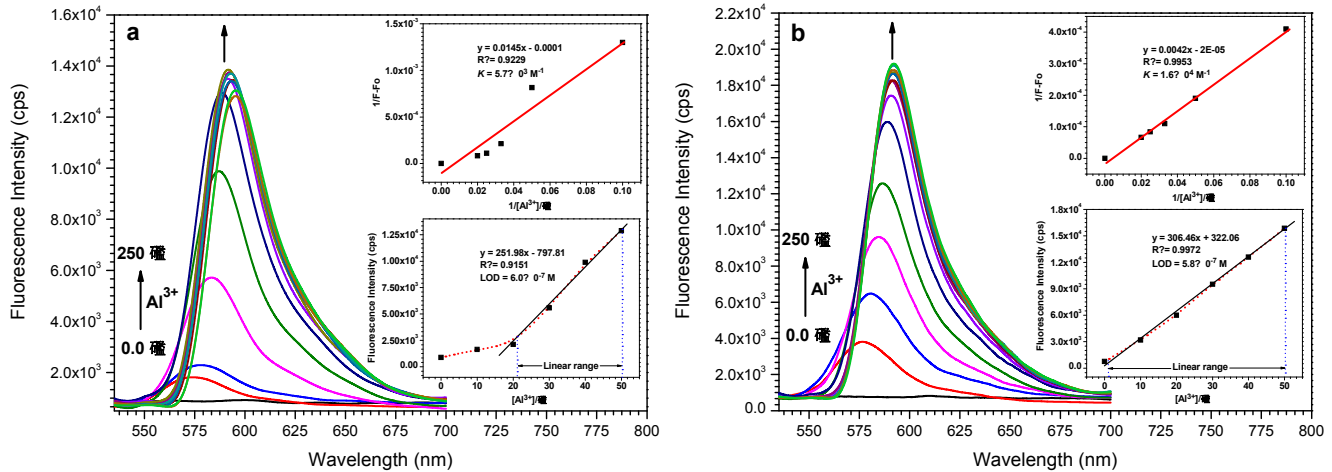


Figure S3. The fluorescence emission spectral pattern of **L1** (a) and **L2** (b) in the presence of increasing concentrations of Al^{3+} (0, 10, 20, 30, 40, 50, 75, 100, 125, 150, 175, 200, 225, 250 μM). Inset: Linear regression plot of fluorescence intensity change $1/(F-F_0)$ as a function of concentration $1/\text{[Al}^{3+}\text{]}$ (top), fluorescence enhancement change as a function of concentration of Al(III) added (bottom).

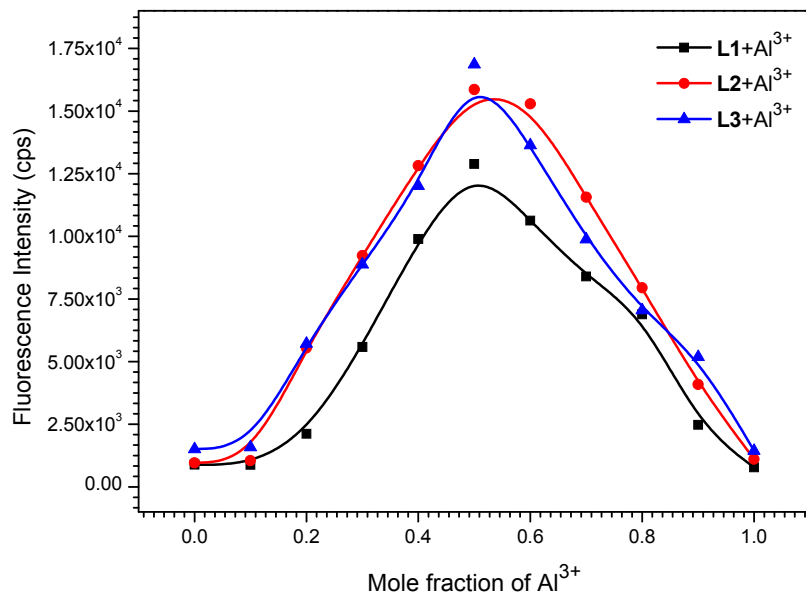


Figure S4. Job's plot for **L1–L3** with Al^{3+} , fluorescence intensity at 587 nm was plotted as a function of the molar ratio.

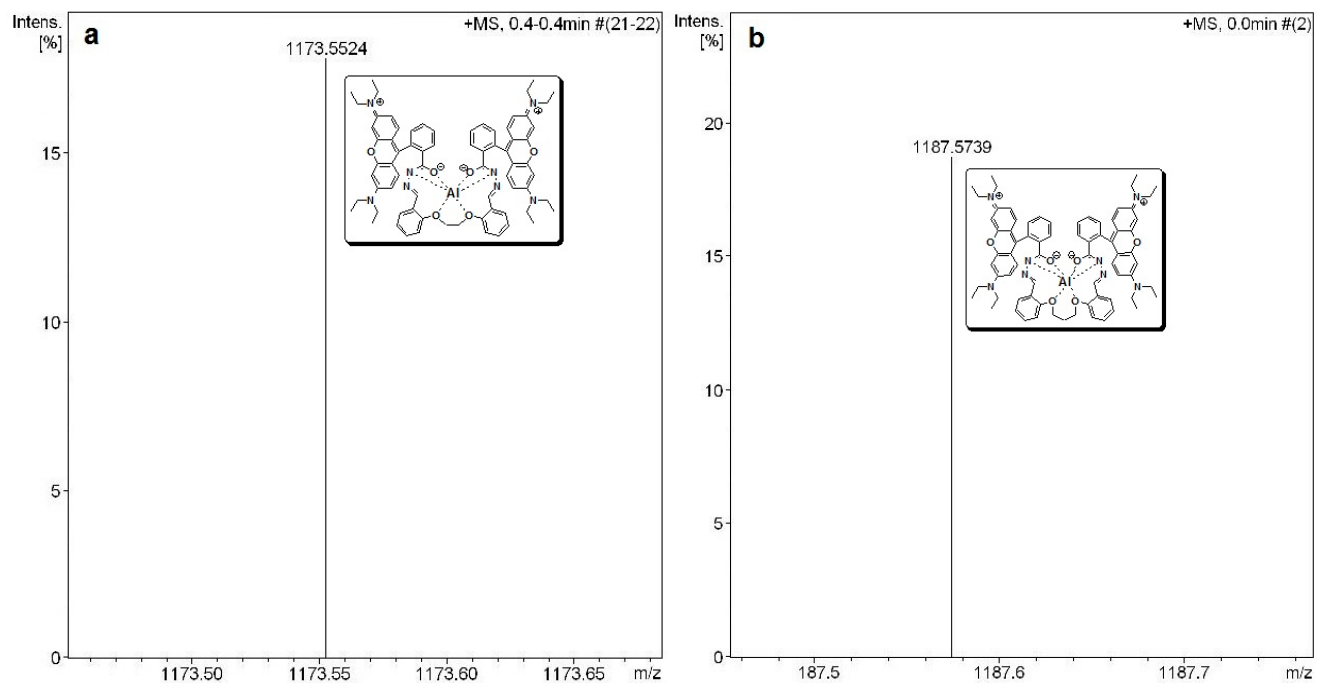


Figure S5. ESI-MS spectrum of **L1** (a) and **L2** (b) upon addition of $\text{AlCl}_3 \cdot 6\text{H}_2\text{O}$ (1.0 equiv.) in MeOH.

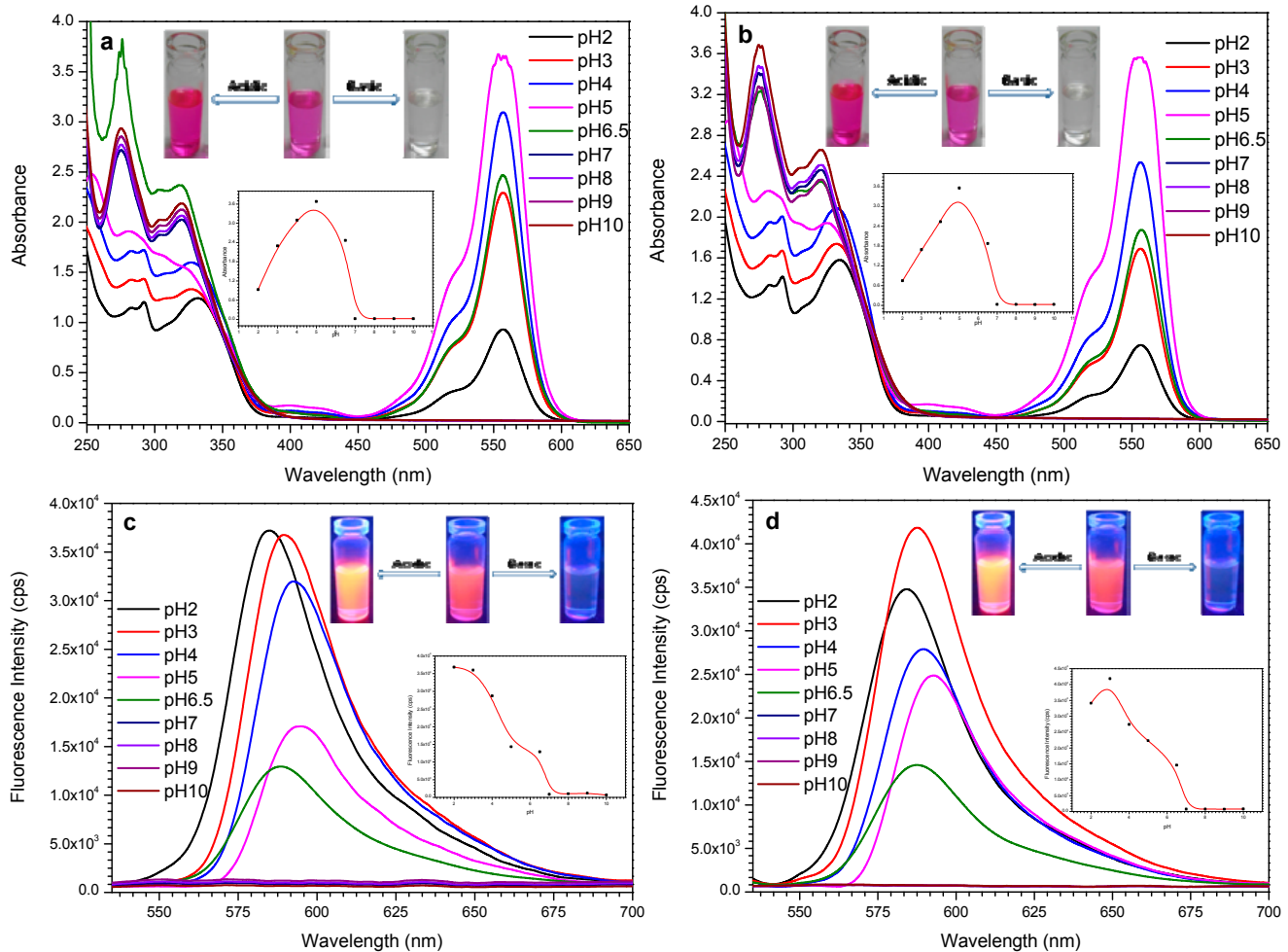


Figure S6. UV-vis absorbance (**a,b**) and Fluorescence emission (**c,d**) spectral changes of **L1** and **L2** with Al^{3+} as a function of pH. Inset: Color changes of probe + Al^{3+} in different pH media under a normal (a and b) and UV (c and d) lamp (top), absorbance (a and b, at 557 nm) and emission (c and d, at 587 nm) intensities of **L1** and **L2** in the presence of Al^{3+} with pH variation (bottom).

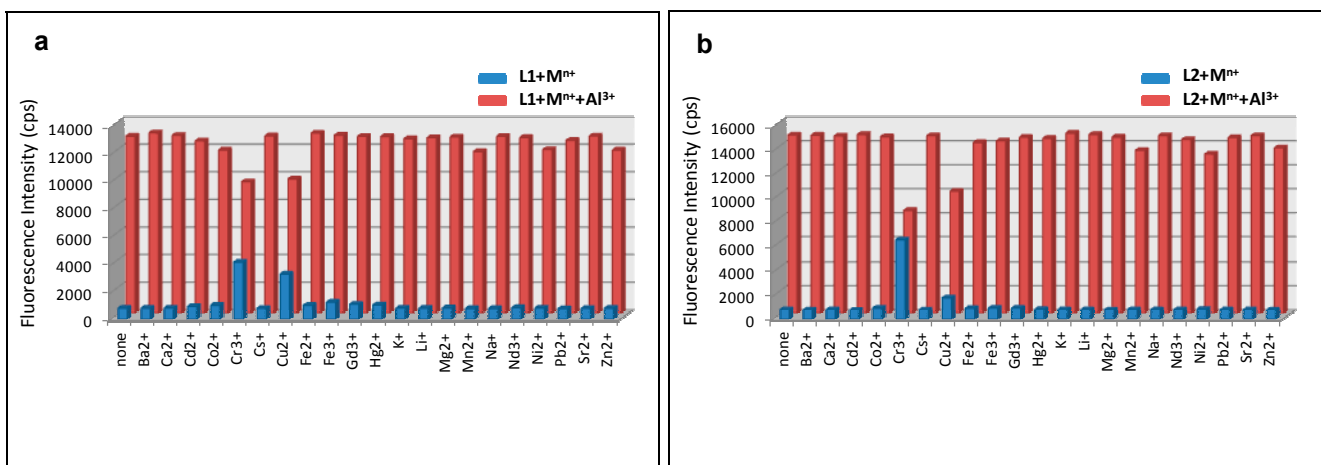


Figure S7. Competitive selectivity of probes **L1** (**a**) and **L2** (**b**) toward various metal ions (1.0 equiv.) in the absence (blue bars) and presence (red bars) of Al^{3+} (1.0 equiv.) with an excitation of 520 nm.

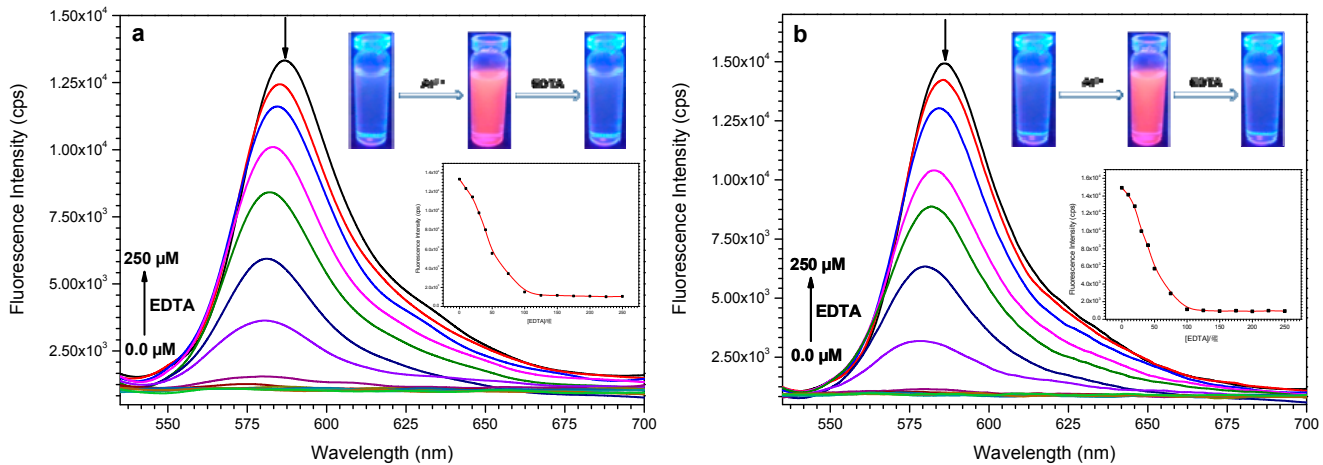


Figure S8. The variation in fluorescence emission spectra of **L1** + Al^{3+} (a) and **L2** + Al^{3+} (b) upon addition of EDTA (0, 10, 20, 30, 40, 50, 75, 100, 125, 150, 175, 200, 225, 250 μM). Inset: Color changes of probe + Al^{3+} upon addition of EDTA (1.0 equiv.) (top), fluorescence spectral changes at 587 nm as a function of the amount of EDTA (bottom).

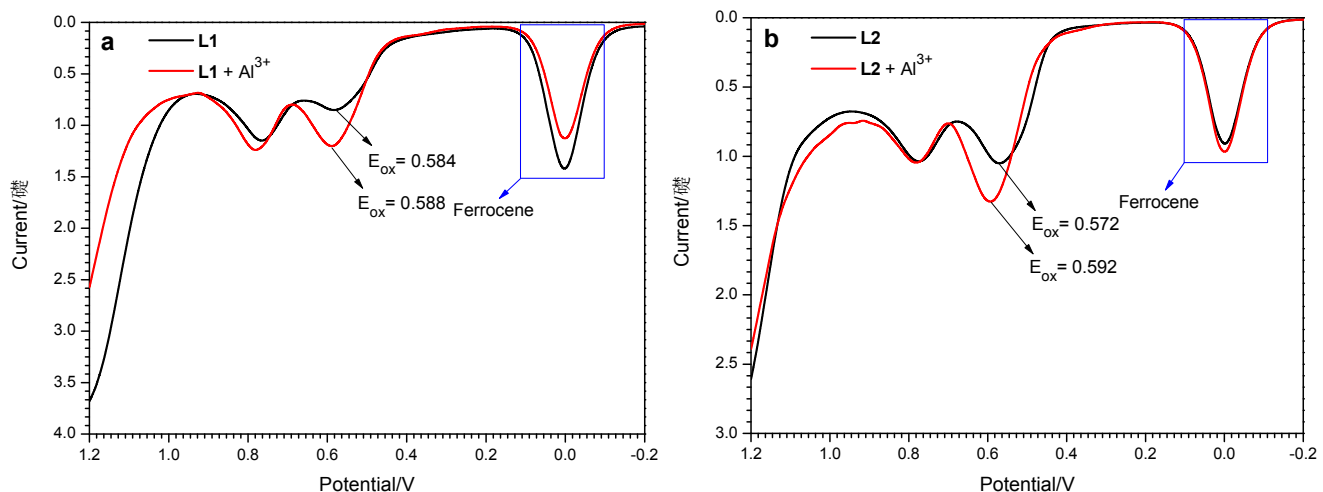


Figure S9. Differential pulse voltammograms recorded for **L1** and **L2**, and the corresponding Al^{3+} addition products in MeOH–DMSO (99:1 v/v).

¹H NMR Titration

Both doublet and triplet of H_j and H_l , respectively, were shifted upfield then they were combined with each other and gave a simple multiplet at about 6.8 ppm, while a combine signal of H_b , H_d and H_i was splitted into two signals of H_i and a combine signal of H_b and H_d . The distance between two signals of H_c and H_k of fluoroionophore **L3** is also varied upon addition of Al^{3+} . Other aryl-proton (H_a) of rhodamine moiety was also shifted slightly downfield because the strong coordination between **L3** and Al^{3+} ion.

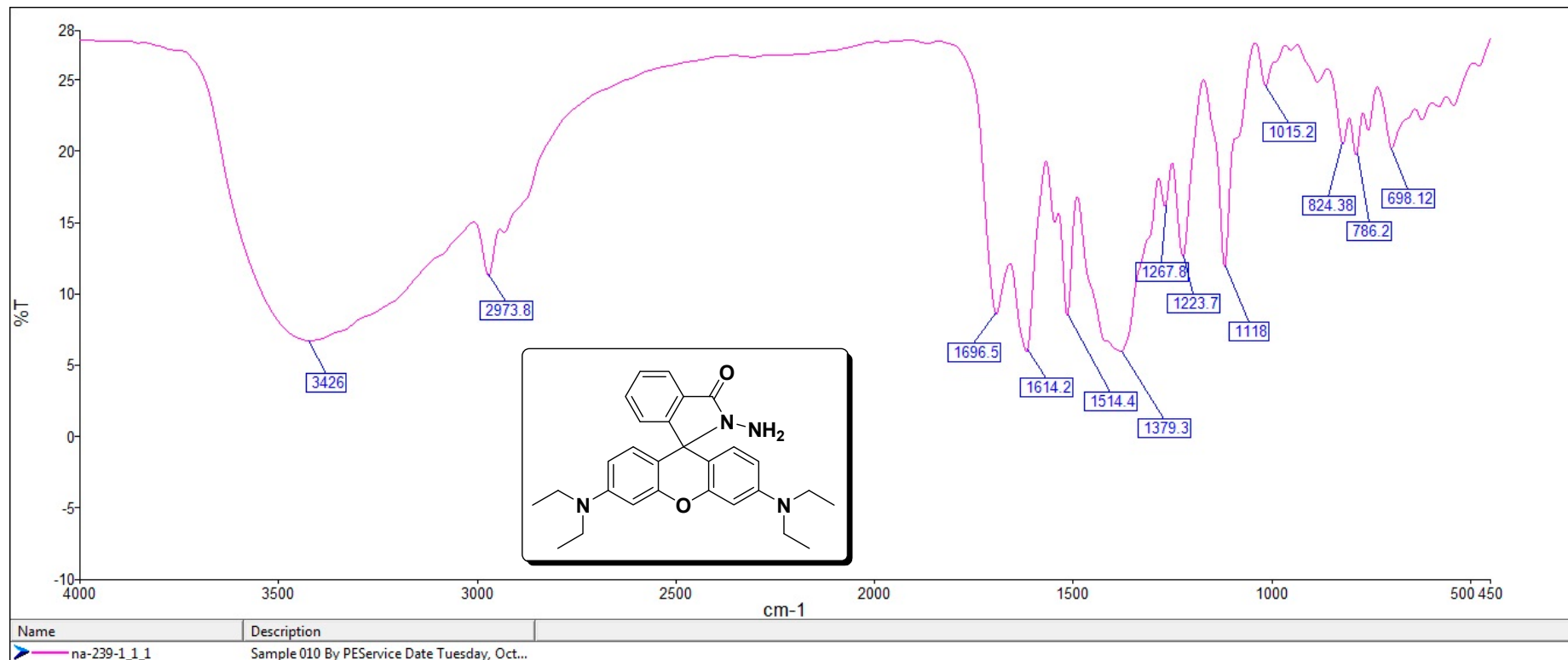


Figure S10. FT-IR Spectrum (KBr) of **1**.

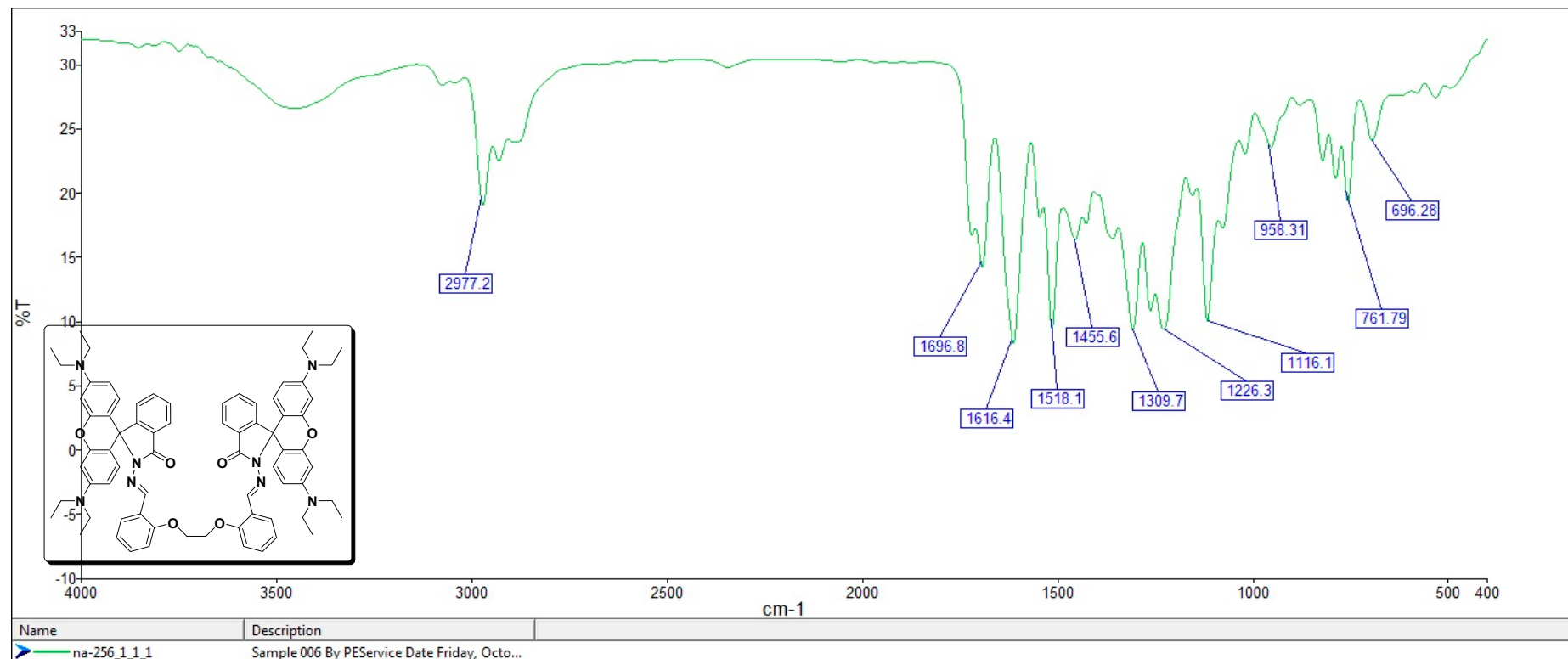


Figure S11. FT-IR Spectrum (KBr) of L1.

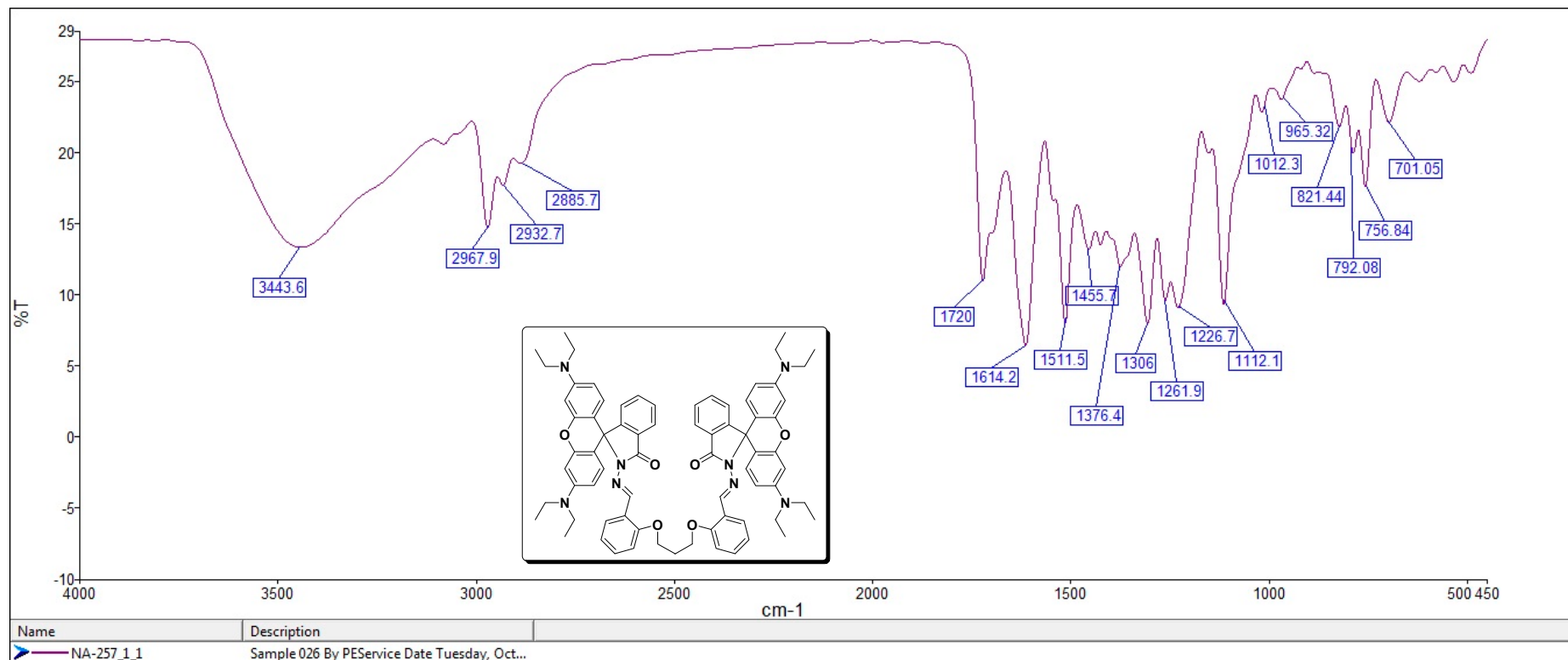


Figure S12. FT-IR Spectrum (KBr) of **L2**.

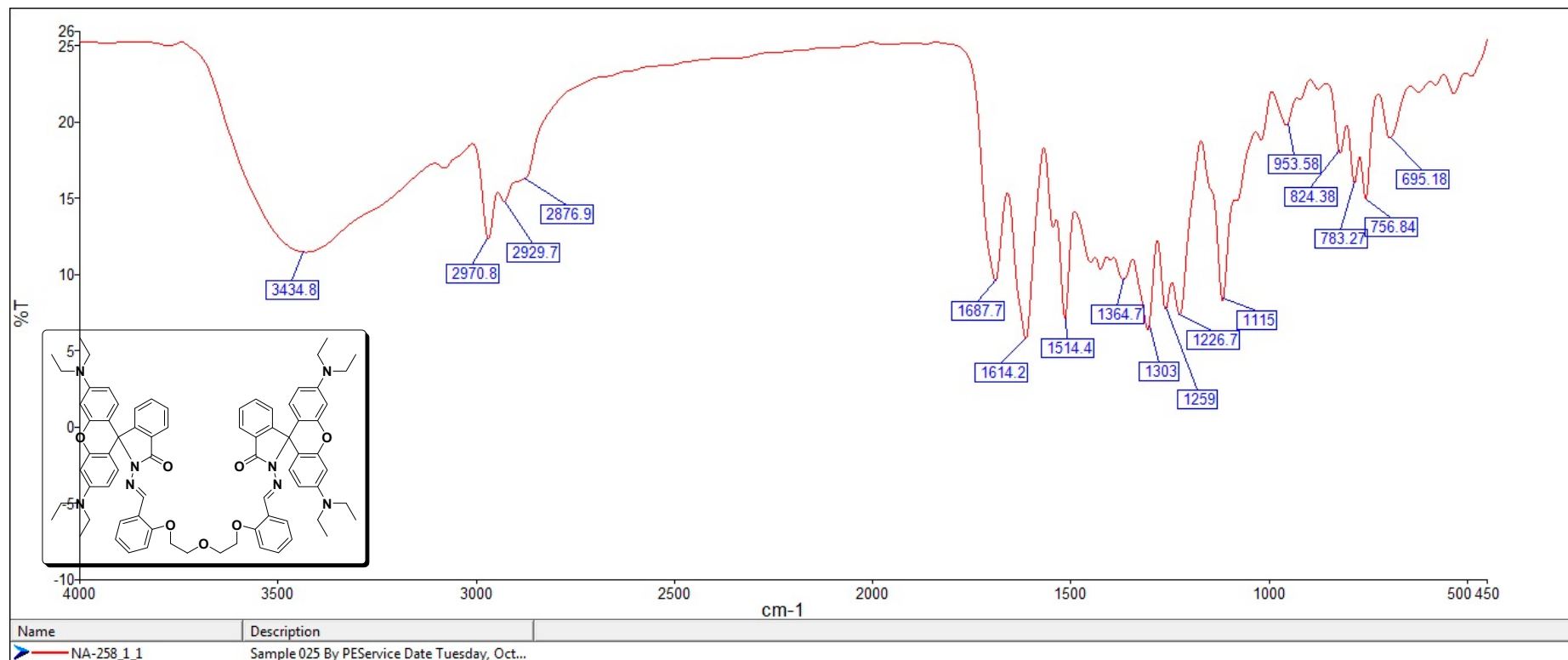


Figure S13. FT-IR Spectrum (KBr) of L3.

Detection Limit

The detection limit was carried out by the following calculations:

$$\text{LOD} = 3\sigma/m$$

where, “ σ ” is the standard deviation of probe (without metal) and “m” is the slope of the plot of fluorescence emission vs concentration of metal.

From the Figure 2b: σ is calculated to be 46.05 and m is 273.44.

$$\text{LOD} = (3 \times 46.05)/273.44$$

$$\text{LOD} = 0.5 \mu\text{M}$$

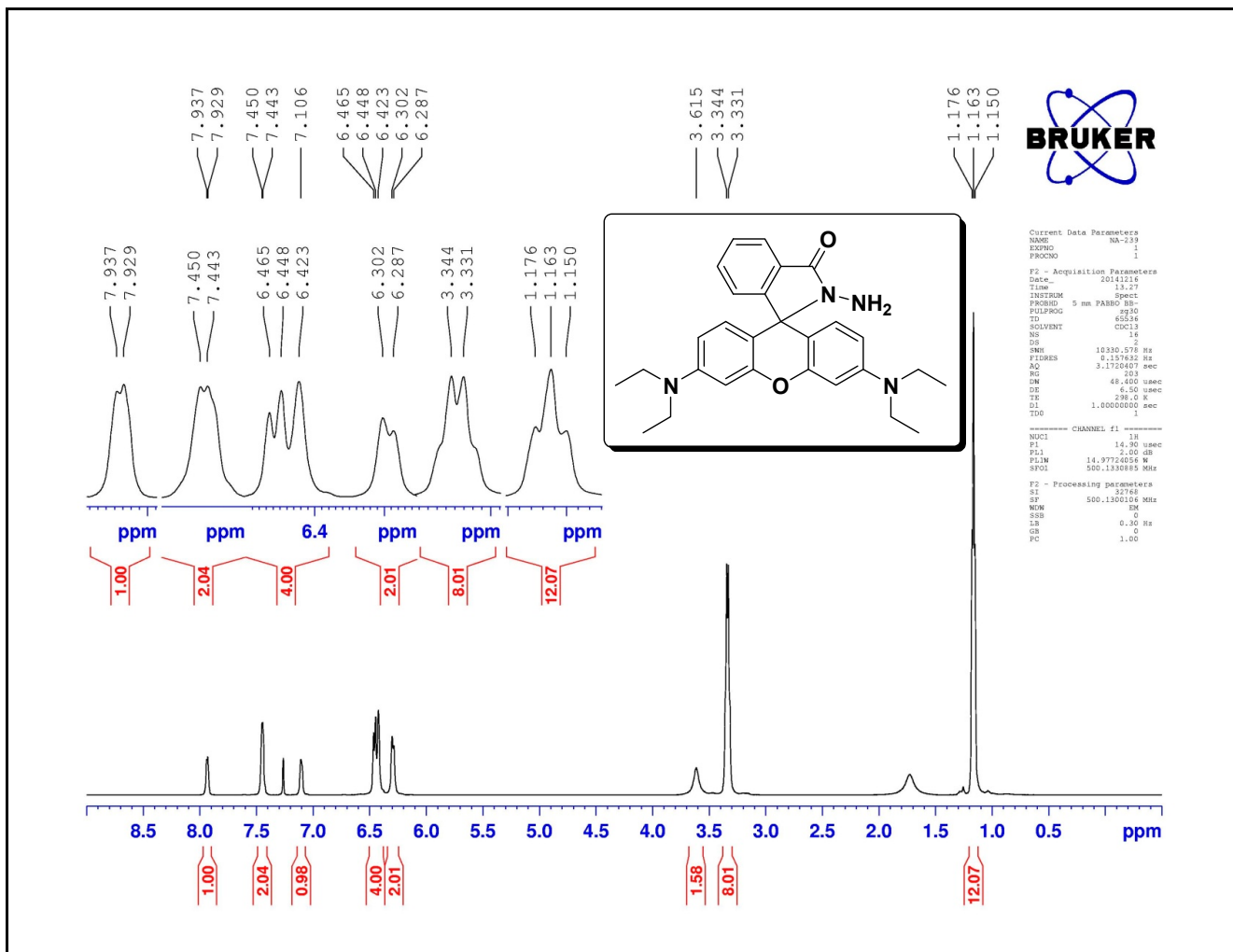


Figure S14. ^1H NMR Spectrum (500 MHz, CDCl_3) of **1**.

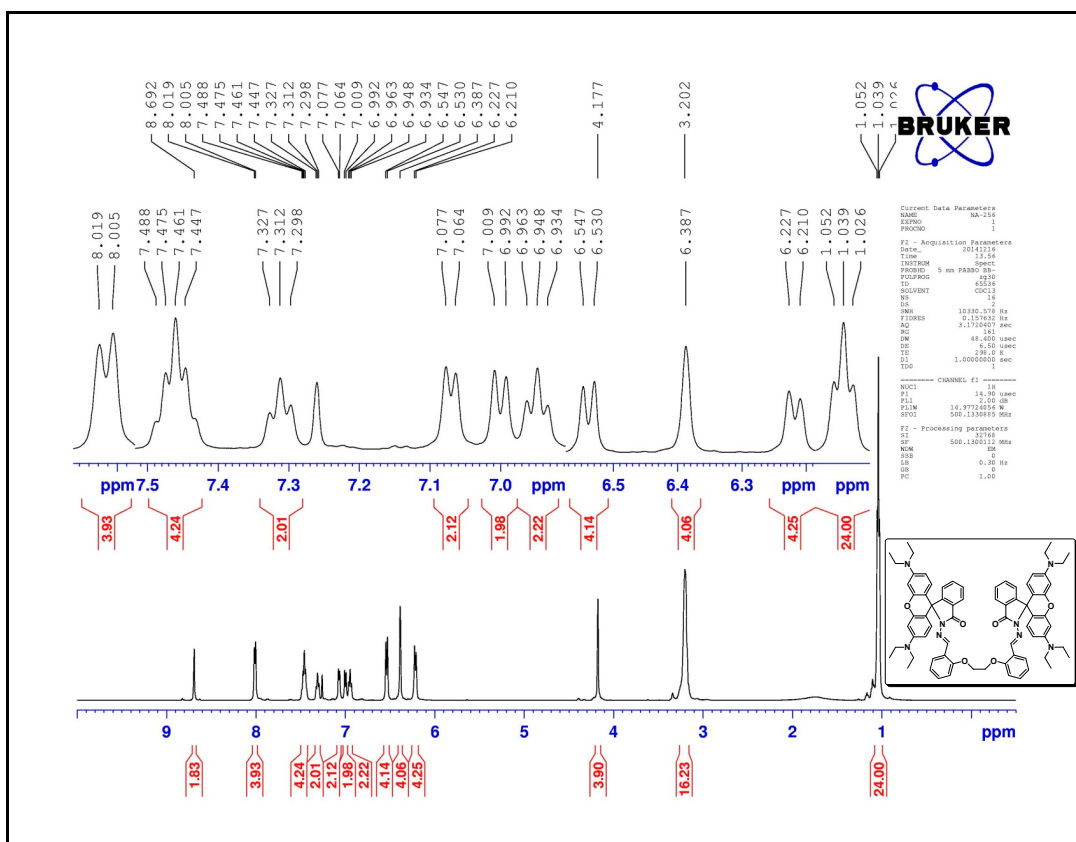


Figure S15. ¹H NMR Spectrum (500 MHz, CDCl₃) of L1.

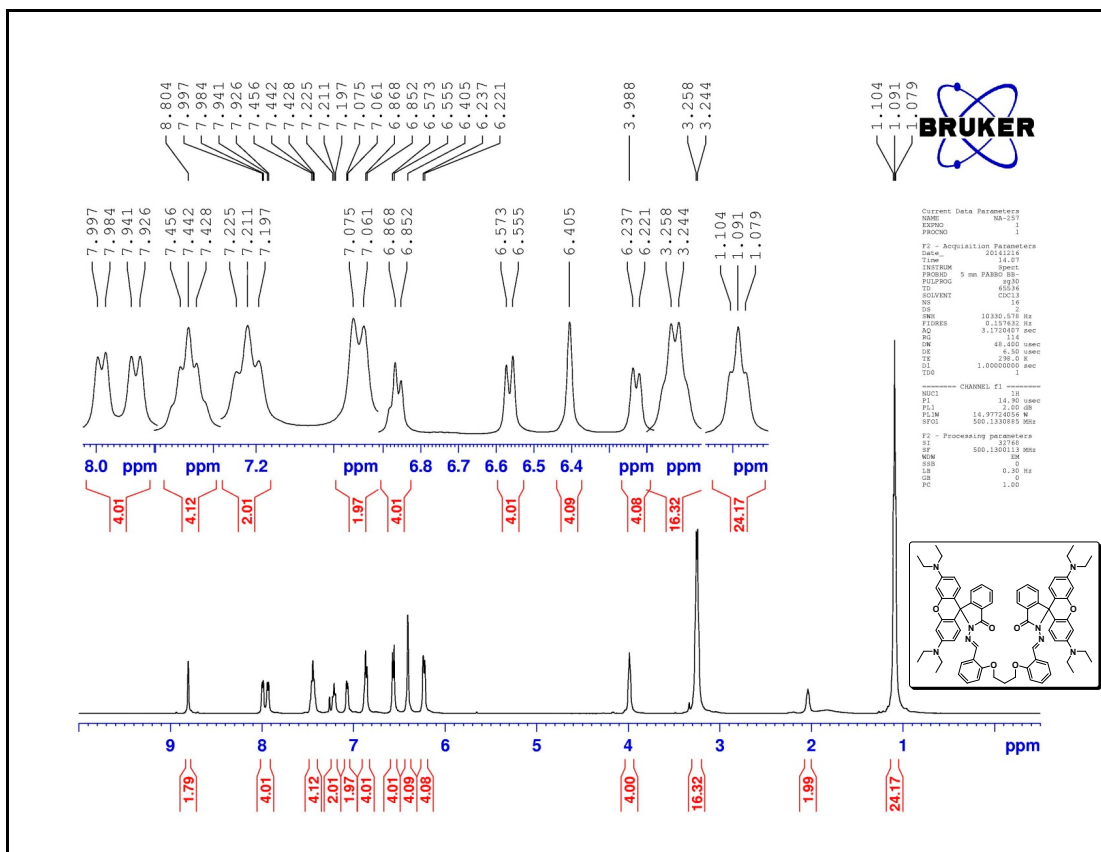


Figure S16. ¹H NMR Spectrum (500 MHz, CDCl₃) of L2.

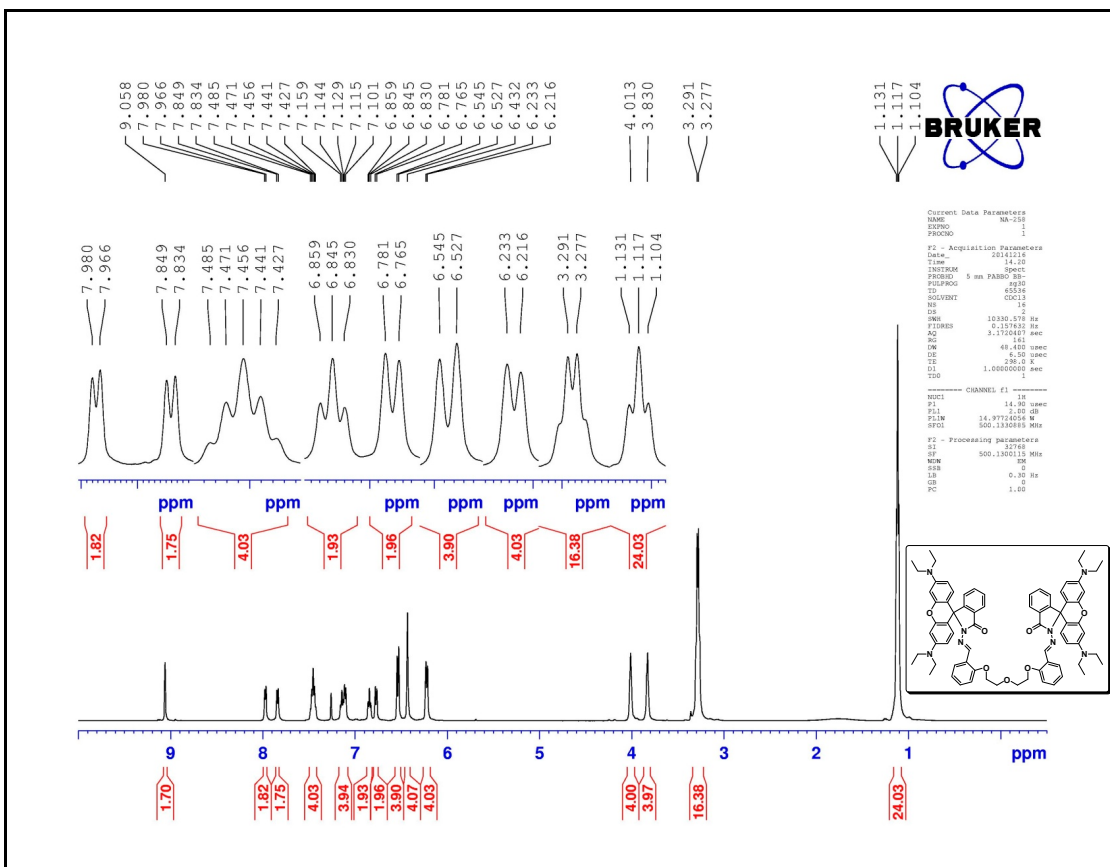


Figure S17. ^1H NMR Spectrum (500 MHz, CDCl_3) of **L3**.

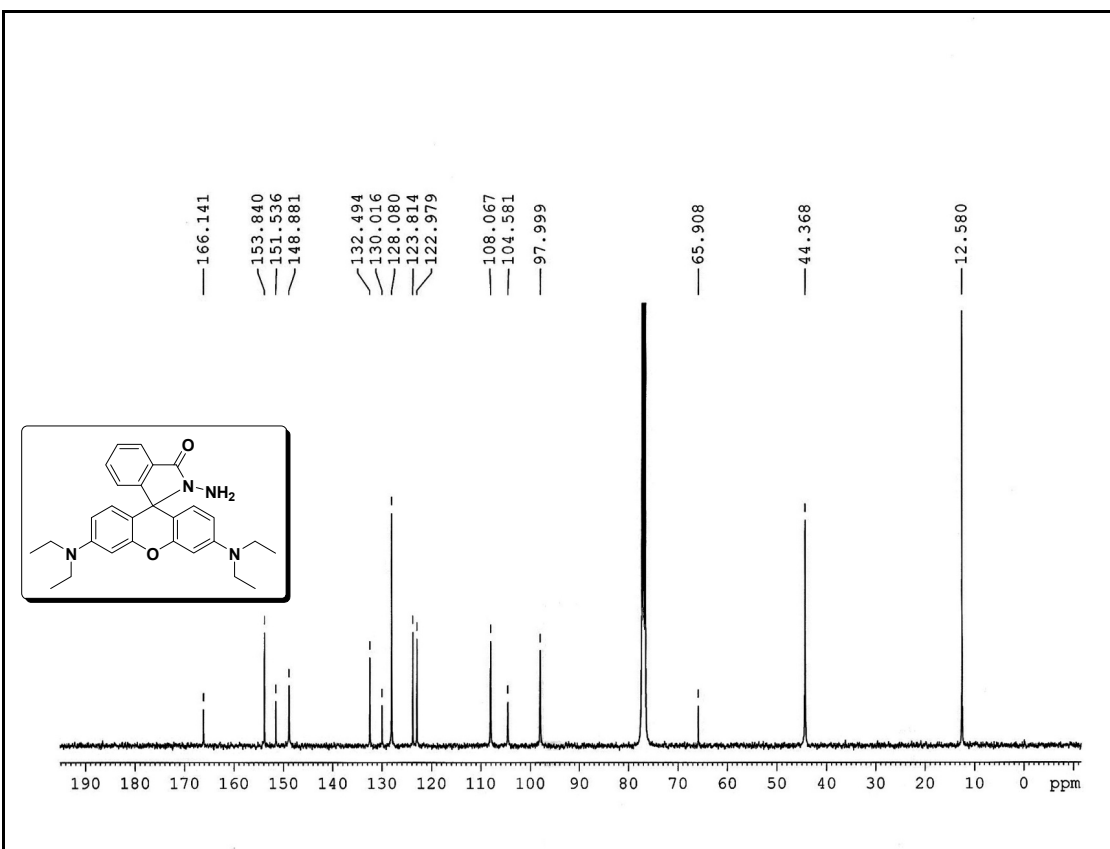


Figure S18. ^{13}C NMR Spectrum (500 MHz, CDCl_3) of **1**.

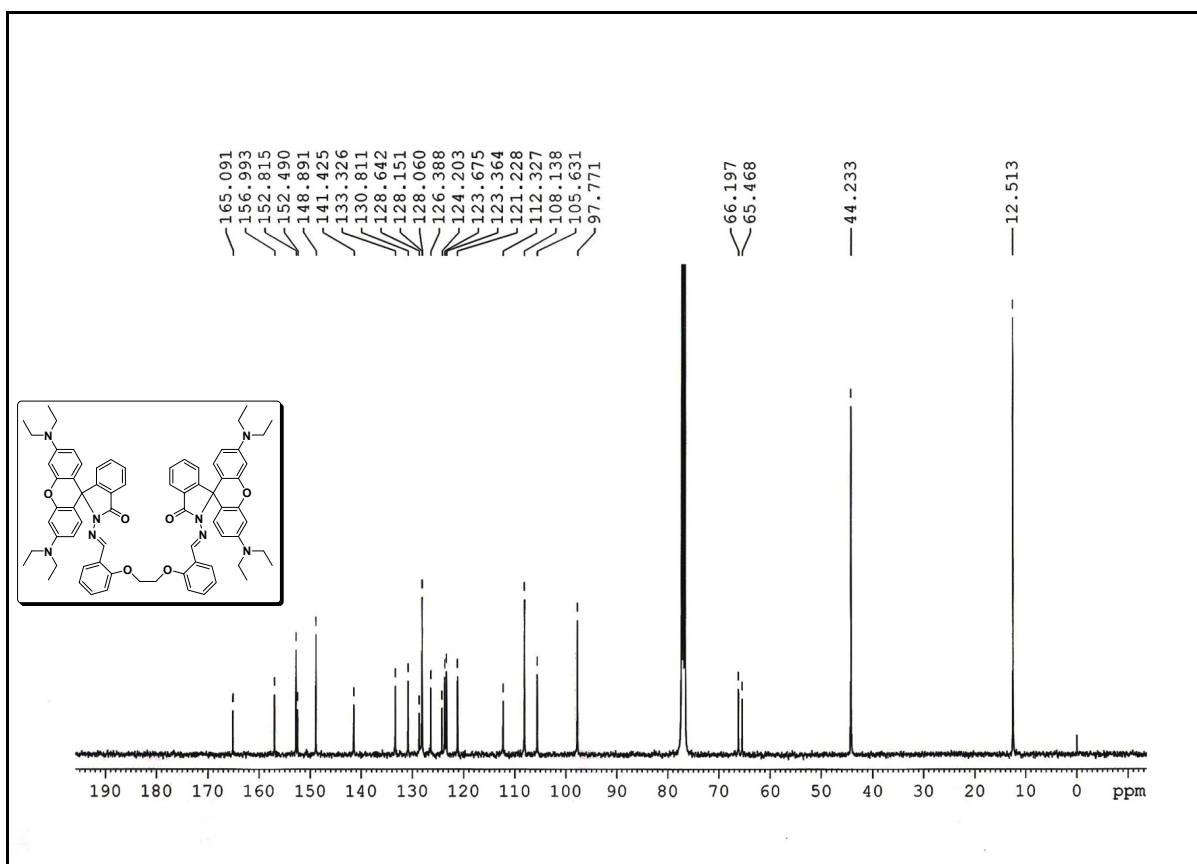


Figure S19. ^{13}C NMR Spectrum (500 MHz, CDCl_3) of **L1**.

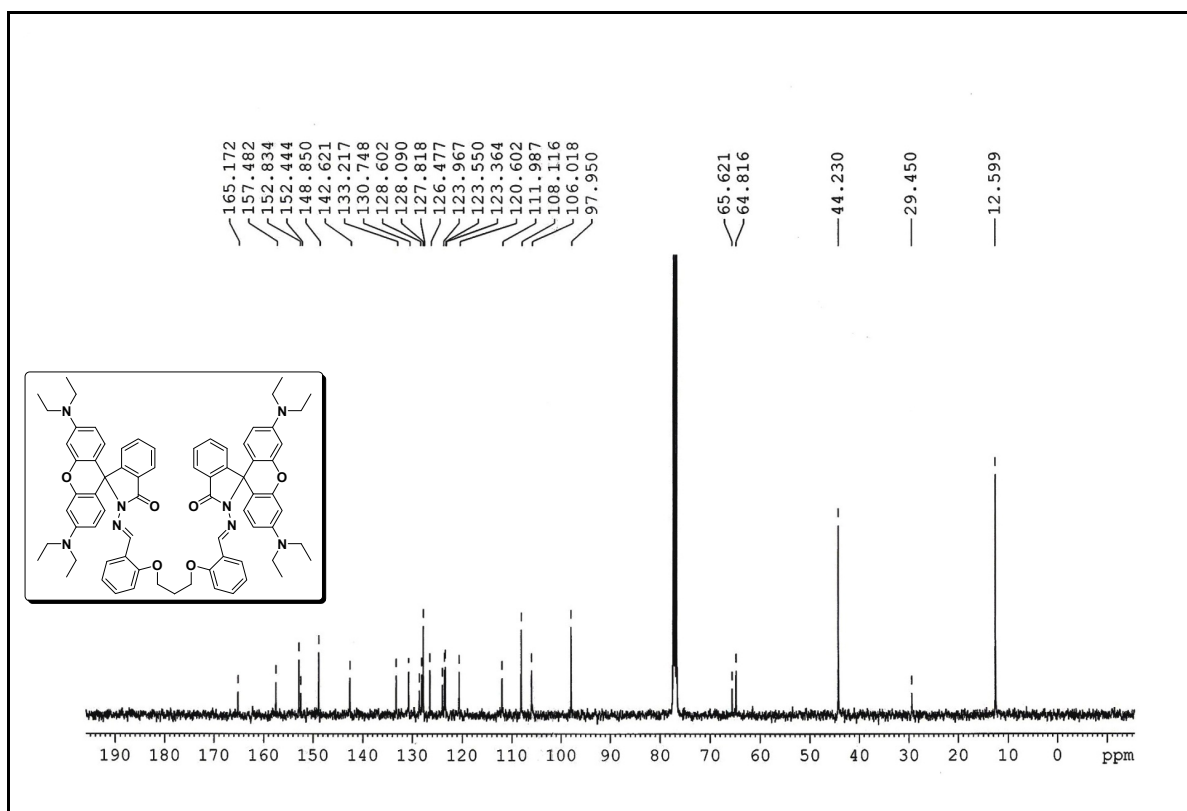


Figure S20. ^{13}C NMR Spectrum (500 MHz, CDCl_3) of **L2**.

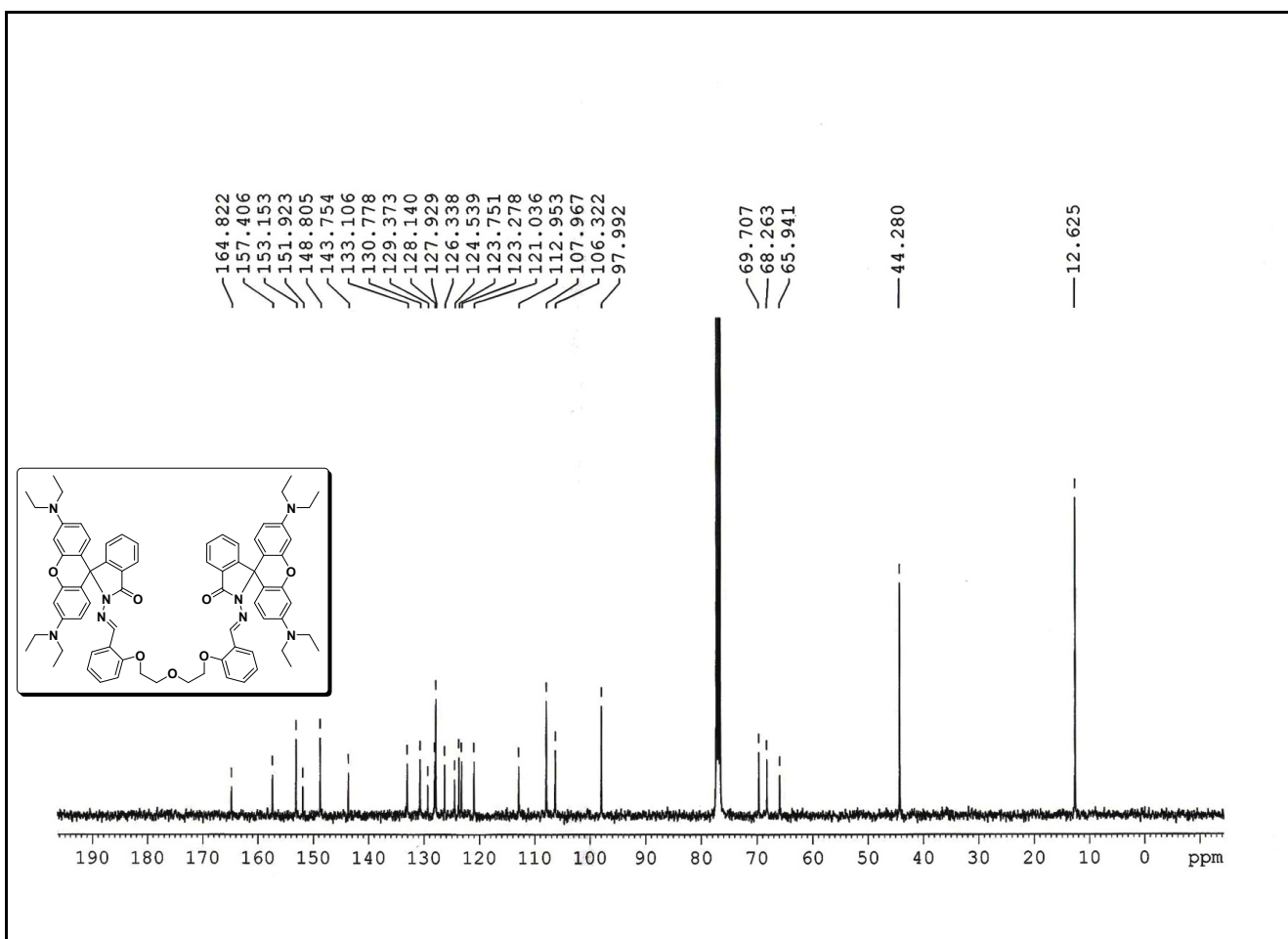


Figure S21. ^{13}C NMR Spectrum (500 MHz, CDCl_3) of **L3**.

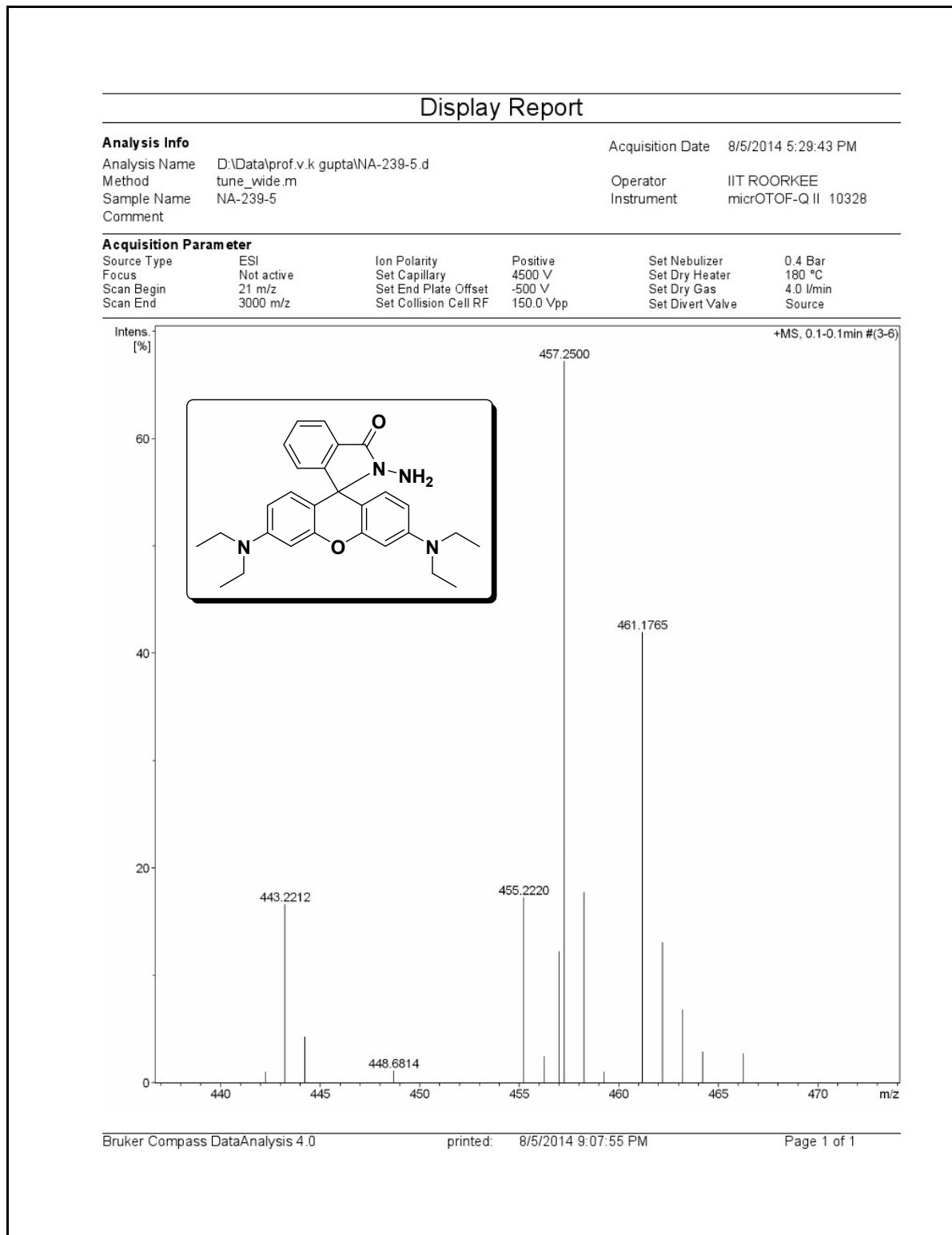


Figure S22. ESI-MS Spectrum of **1**.

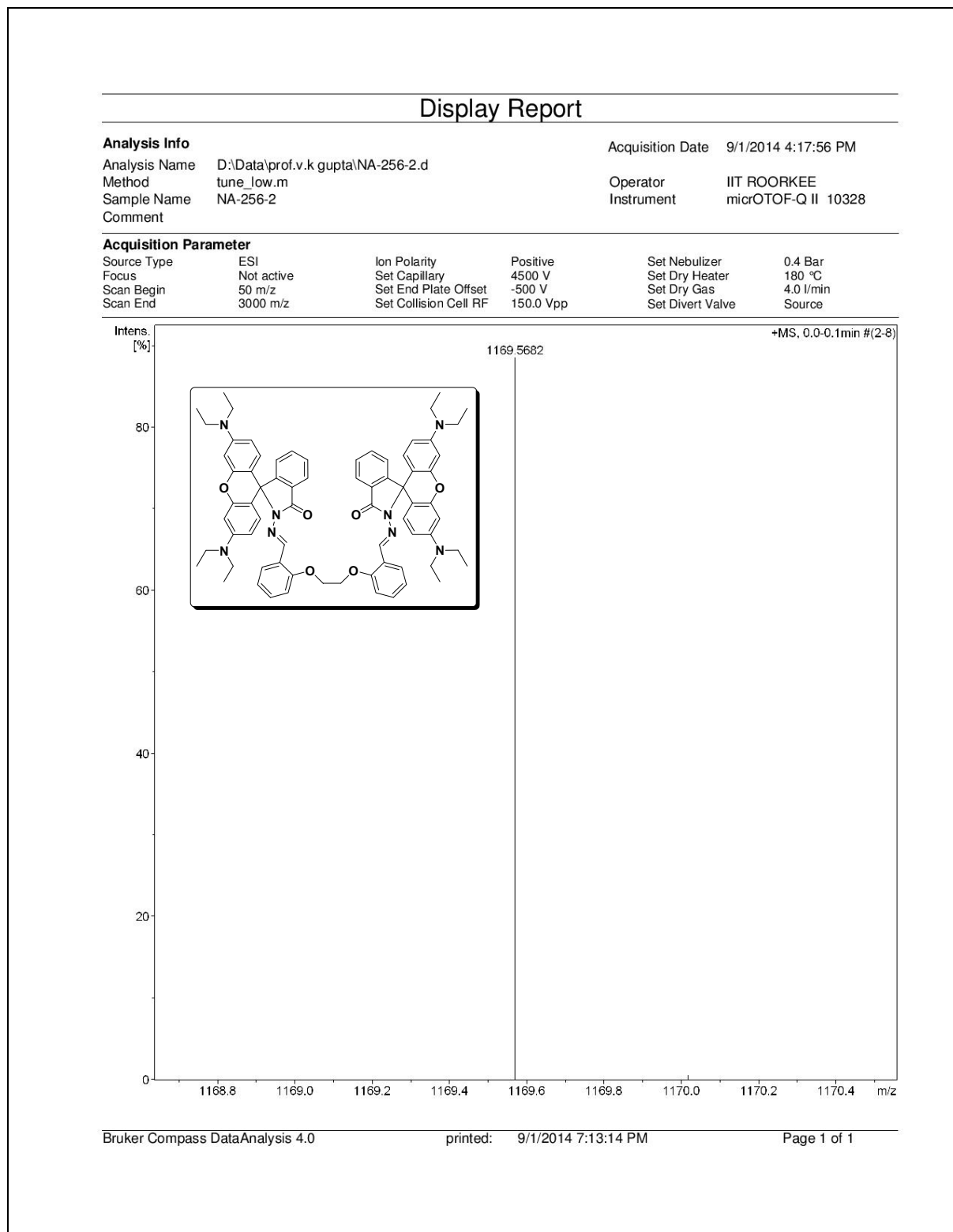


Figure S23. ESI-MS Spectrum of L1.

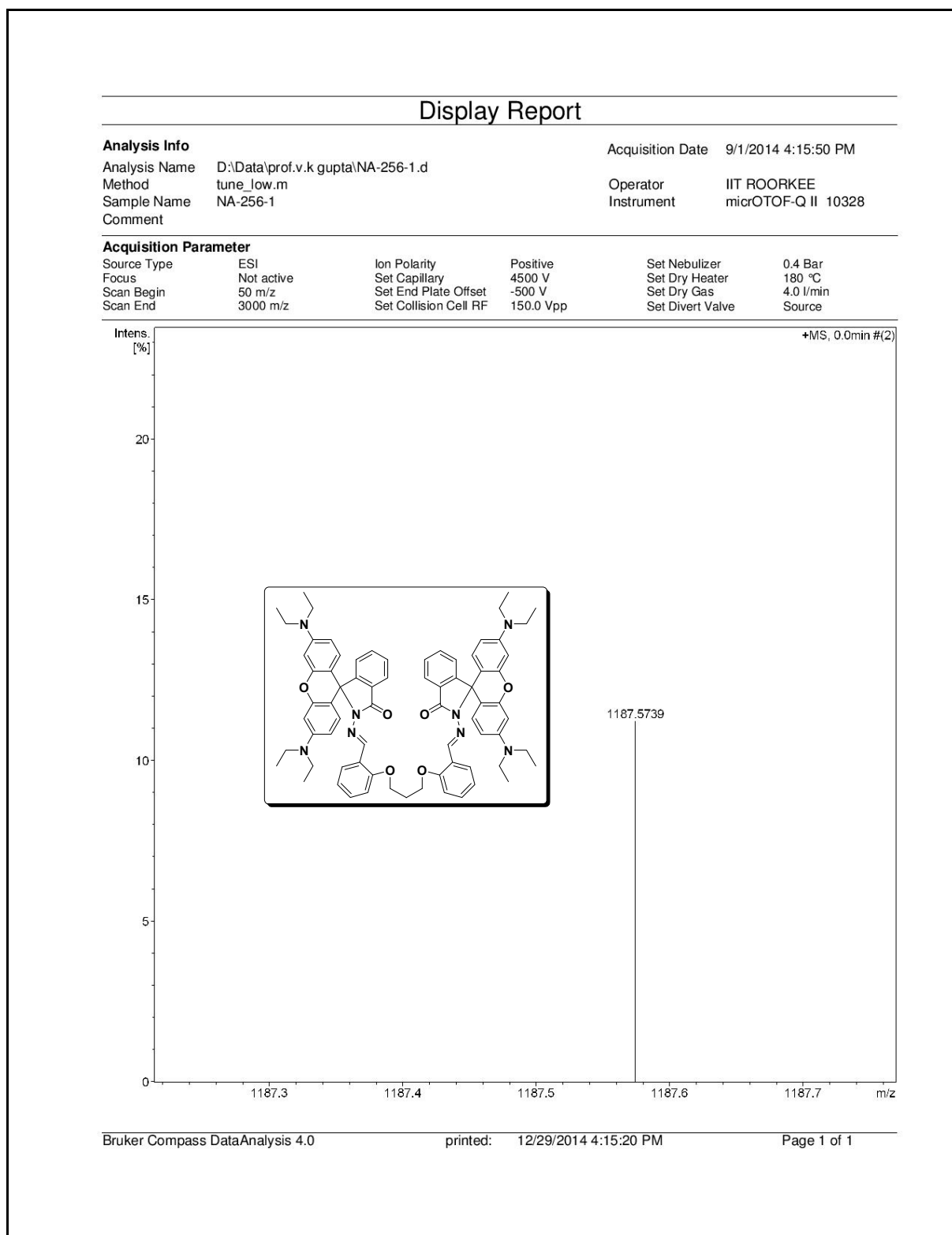


Figure S24. ESI-MS Spectrum of L2.

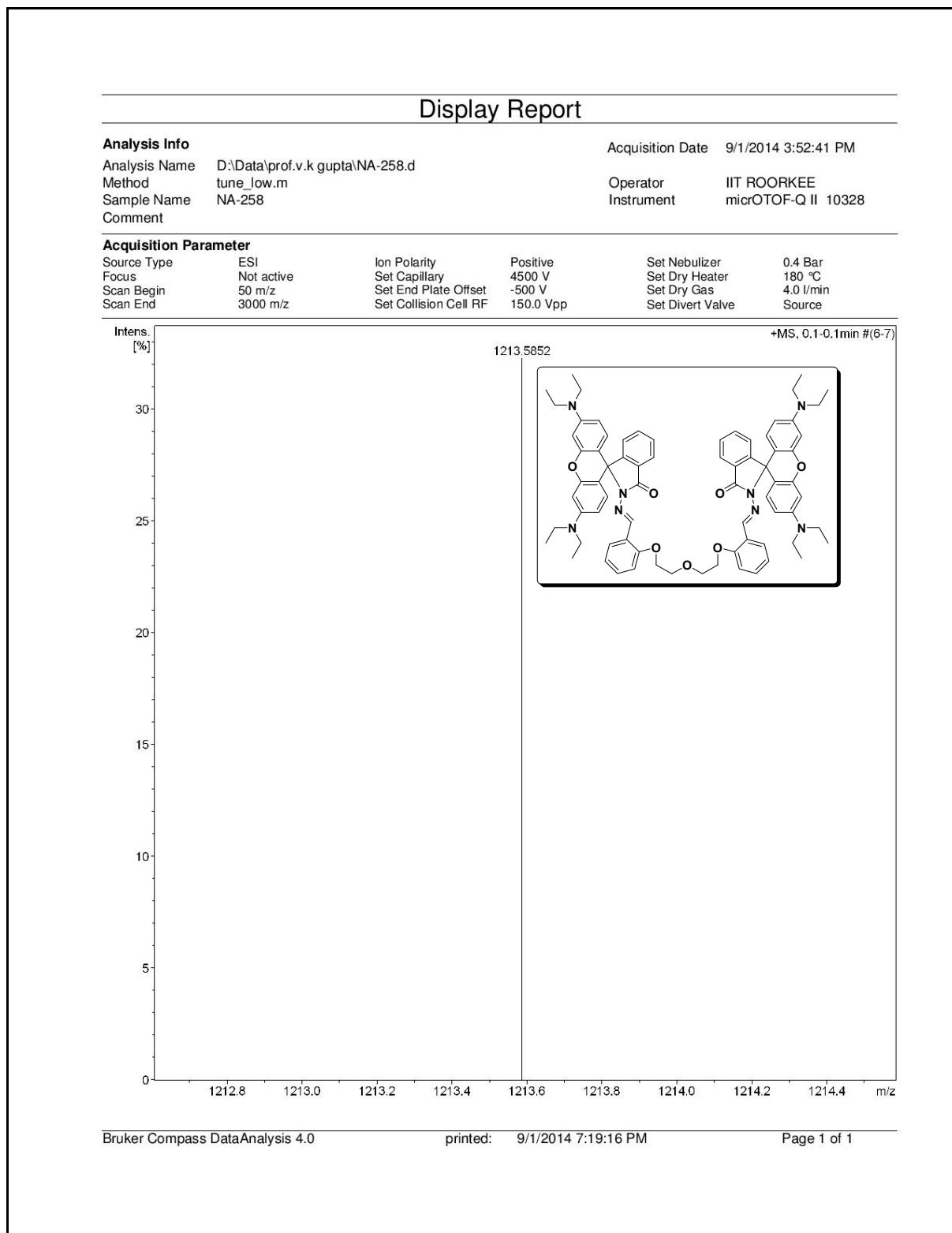


Figure S25. ESI-MS Spectrum of L3.

© 2015 by the authors; licensee MDPI, Basel, Switzerland. This article is an open access article distributed under the terms and conditions of the Creative Commons Attribution license (<http://creativecommons.org/licenses/by/4.0/>).